Stark effect of confined shallow levels in phosphorus-doped silicon nanocrystals

A. Debernardi[1] and M. Fanciulli[1,2]
[1]*Laboratorio MDM, IMM-CNR, via Olivetti 2, I-20041, Agrate Brianza, Italy*
[2]*Dipartimento di Scienza dei Materiali, Universitá degli Studi Milano-Bicocca, 20125 Milano, Italy*
(Received 6 October 2009; revised manuscript received 12 February 2010; published 4 May 2010)

By envelope-function approximation, we computed the effect of confinement in spherical P-doped Si nanocrystals in a uniform electric field without adjustable parameters. Based on nanocrystal size, we can distinguish several regimes. For a radius R that is larger than R_t ($R_t \sim 21$ nm) the ground state is ionized at a critical electric field, $\mathcal{E}_{cr}$, by tunneling from a $1s$-like state, localized at the impurity, to a $2p$-like state, localized to the well that is formed by the electric field and the potential barrier that is generated by the embedding matrix at the nanocrystal surface. For smaller nanocrystals, for which $R_{sp} < R < R_t$ ($R_{sp} \sim 7$ nm), there is a range of electric fields in which the ground state is formed by the hybridization of the impurity states and surface-well states. Further, within this hybridization range, there is a value of the electric field at which the ground $1s$-like state and the excited $2p_0$ state have the same hyperfine coupling. Based on these findings, we envisage a quantum computing scheme in which qubits shuttling relies on excited states when an electric field is applied.

DOI: 10.1103/PhysRevB.81.195302 PACS number(s): 71.70.Ej, 03.67.Lx, 73.22.−f

I. INTRODUCTION

Crystalline silicon, doped with P impurities, is one of the most commonly used materials in electronics and in the past several decades, it has been the focus of many studies.[1] P-doped crystalline silicon has recently attracted renewed interest due to the development of novel technological applications, such as the terahertz laser,[2] and the quantum computer.[3,4] If the latter application is built successfully, it will revolutionize information science technology. In fact, a computer that obeys the laws of quantum mechanics promises to exceed the capabilities of the classical computer, particularly with regard to factorization problems that have important implications for cryptography. In 1998, Kane proposed a model in which quantum bits (qubits, for short) are stored in the nuclear spin of P atoms in crystalline silicon.[3] The qubit interaction between two P atoms is mediated by the electron in shallow states of P whose wave function, for the P atom in Si, extends for several nanometers. The coupling between the nuclear spin and the electron spin of the shallow state is determined primarily by contact hyperfine interaction, which is proportional to the square modulus of the electron wave function at the nuclear site. Qubit operations may be performed by manipulating the shallow electron wave function with an electric field, therefore tuning the hyperfine interaction (single qubit operation) or the exchange interaction (qubit-qubit coupling) between shallow electron states of different P atoms. In this context, the Stark effect is of paramount importance because it describes the dependence of the energy level on a uniform electric field. Several theoretical studies have addressed the Stark effect in bulk silicon that is doped with shallow donors[5–10] and some recent papers have considered the Stark effect for donors in the presence of an interface.[11–15]

In the same year of Kane's proposal, Loss and Di Vincenzo proposed a different scheme in which the qubit is stored in the spin of the electron that is confined in a quantum dot.[4] Here, we consider a system that combines aspects of both proposals, studying P-doped silicon nanocrystals (NCs). This system can be simulated ab initio for small NCs (e.g., see Ref. 16, which reports first-principles simulations of Si dots that are up to 3 nm in radius). Computations of quantum-confinement effects over a large range of crystals sizes—i.e., on the order of 10 nm—are beyond the present computational capabilities of first-principles simulations. Therefore, less time-consuming techniques are necessary. In this study, we used a method that is based on the envelope-function approximation to compute the Stark effect in Si-NCs whose radii range from 5 to 30 nm. This method has recently been developed to simulate, without adjustable parameters, shallow electron levels of P impurities in bulk silicon[10] and Si nanostructures.[17,18] The theoretical results are consistent with experimental data that have been obtained at zero electric field.

Examination of the Stark effect in P-doped Si-NC as a function of NC radius (R) revealed that for R larger than $R_t \sim 21$ nm, the donor is ionized at the critical field by tunneling from a state in which the electron is confined in the potential well, which is formed primarily by the coulomb potential of the donor, to a state in which the electron is confined at the surface of the NC in the potential well that is formed by the electric field. This mechanism is similar to the one that is predicted in bulk Si:P (Ref. 10) in which the donor is ionized at the critical field by tunneling.

For $7 \text{ nm} < R < 21$ nm, we observed a range of electric fields in which the ground state is a "hybrid" of an s-like state that is partially localized at the impurity and a p-like state that localizes partially in the well at the surface of the NC. Notably, within this hybridization range, there is an electric field value at which "both" the ground and one (or more) excited states can have similar (or, in some cases, identical) hyperfine couplings (HFCs), theoretically allowing the use of excited states to transfer quantum information in quantum computation schemes that store qubits in nuclear and electronic spin.

Hybrid states are also observed near the P-doped silicon/SiO_2 interface. In fact, in the presence of an electric field, the ground state is a hybrid of states that are localized at the impurity and a state that is confined in a well that is

formed by the electric field and the barrier at the interface (see Refs. 19 and 20 and references therein).

This paper is organized as follows. In Sec. II, we introduce the approximation that is used and give a brief account of the computational technique. In Sec. III, we present our data on the Stark effect in Si-NCs. In Sec. IV, we discuss the physical behaviors of various-sized NC. In Sec. V, we discuss the confinement effect on HFC and propose a scheme to shuttle the qubit from an NC to an adjacent one.

II. PHYSICAL APPROXIMATIONS

We consider a single impurity atom per NC, a condition that can be realized experimentally.[21,22] In this case, the Hamiltonian of a substitutional impurity in the presence of a uniform electric field, $\mathcal{E}$, reads

$$H_0 + V_{imp} - |e|\mathcal{E}\cdot\mathbf{r} + v_{matr}(\mathbf{r}), \tag{1}$$

where V_{imp} is the donor impurity potential and includes all of the effects that are caused by the presence of the guest atom in the crystals, H_0 is the periodic Hamiltonian of the host crystal, and v_{matr} is the potential barrier at the NC surface due to the matrix that embeds the NC. We consider spherical NCs (Ref. 23) that simulate the shape that is observed experimentally in P-doped Si-NC in an SiO_2 matrix (see, e.g., Refs. 22 and 24). In this case, we can conveniently approximate the potential barrier at the surface of the NC with a spherical well,

$$v_{matr}(\mathbf{r}) = \begin{cases} 0; & \text{if } \mathbf{r} \le R \\ V_0; & \text{if } \mathbf{r} > R, \end{cases} \tag{2}$$

where R is the radius of the NC. In our simulation, we chose V_0=3.2 eV for the value of the barrier height (i.e. of the confinement potential), which corresponds to the experimental value of the conduction-band offset of the Si/SiO_2 interface.[25] In our calculations the P atom is placed at the center of the NC. According to the first-principles simulation of Ref. 16, the assumption of P at the center corresponds to the minimum-energy configuration of the P atom in Si-NCs for which $R>1$ nm 26 (for $R<1$ nm, the energetically favored configuration places the P atom at the surface of the NC).

When nonthermodynamic processes are employed to synthesize an experimental sample, the donor can also occupy nonequilibrium positions and the donor can be detected in noncenter sites. Nevertheless, we expect that our results, obtained under the assumption of a central P, can also describe the behaviors of the energy levels as a function of the electric field for noncentered donor, at least qualitatively, provided that the distance of the donor from the center is small compared with the radius of the NC. In fact, with the same method used in the present work, we reproduced the dependence of the HFC on the radius of P-doped Si-NCs,[21] within experimental error and without adjustable parameters,[17] under the assumption of a P that was centered in the Si-NC.

The shallow electron wave function was computed within the envelope-function approximation,[27] according to the scheme in Ref. 10. This technique takes into account the anisotropy of the effective mass, the valley-orbit interaction, and the contribution to the central-cell correction due to the core state of P—the so-called *core correction*. The envelope function was expanded on a Gaussian basis set. The basis that was used in the present calculation (approximately 1800 Gaussian basis set) is the same used in Refs. 17 and 18 to compute the shallow state of Si-NC at zero electric field. The interested reader can refer to these papers for further technical details.

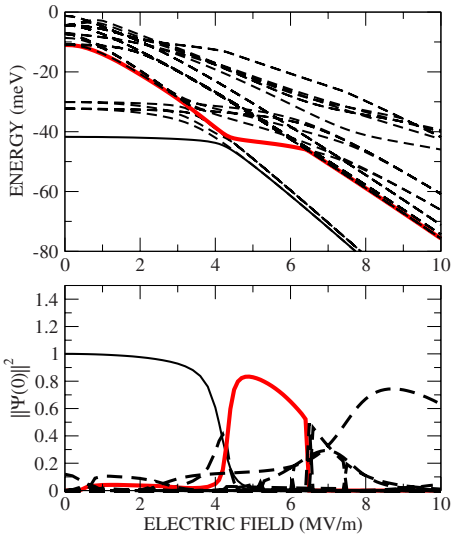

FIG. 1. (Color online) Top panel: the lowest energy levels (solid lines) of a Si:P nanocrystal with a 20 nm radius. Bottom panel: the square modulus of the corresponding wave functions computed at the impurity site and normalized to the value of the bulk system at zero field. A (black) solid line denotes the ground state, a (red) thick solid line denotes the lower energy level of the $2p$ manifold, and dashed (black) lines denote the other energy levels.

III. STARK EFFECT IN Si-NC

First, we studied the effect of confinement on energy levels and the HFC as a function of electric field. In Figs. 1–4, we show our results for the Stark effect due to a uniform electric field that is oriented along the [001] direction for an NC of R=20, 15, 10, and 5 nm, respectively (the same results can be obtained with an electric field that is applied along the [010] and [100] directions, equivalent by symmetry). Hereafter, the zero of the energy (vertical scale in the figures) corresponds to the bottom of the conduction band. For a given value of an electric field $\mathcal{E}$, the energy levels are computed with respect to the corresponding conduction-band minima at $\mathcal{E}$ because the difference in energy levels with respect to the conduction-band minima is the quantity of interest. Negative-energy levels correspond to discrete states that are bound to the donor. Positive-energy levels are superimposed onto the conduction band and correspond to states that are delocalized within the entire NC.

In the top panel of each figure, we show the lower energy levels of the shallow electron as a function of the electric field and in the bottom panel are the corresponding HFC parameters (contact interaction only), which are proportional

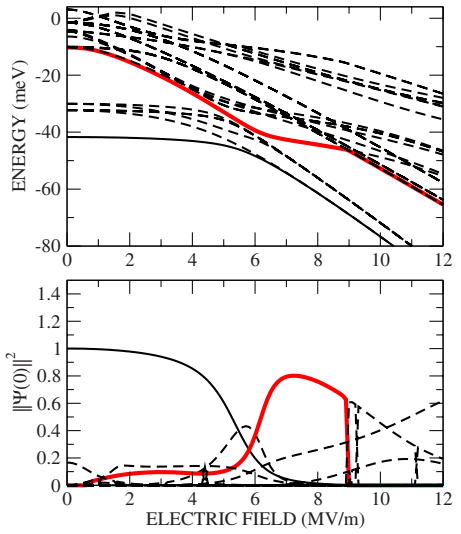

FIG. 2. (Color online) The same as Fig. 1 but for a nanocrystal with a 15 nm radius.

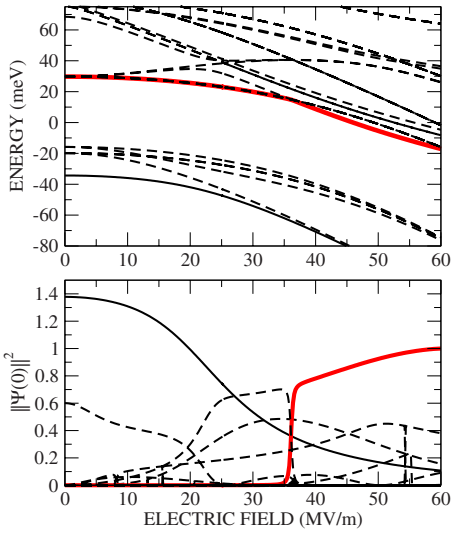

FIG. 4. (Color online) The same as Fig. 1 but for a nanocrystal with a 5 nm radius.

to the squared modulus of the electronic wave function at the nuclear site of the P atom. The latter quantities are of paramount importance in any quantum information processing scheme that is based on donor electron or nuclear spin in silicon.

The effect of confinement can be gleaned immediately from the figures. In general, the value of the HFC of the ground state at zero field increases as the NC radius decreases. This effect becomes appreciable for NCs with $R \leq 8$ nm and corresponds to an increase in ground-state energy due to confinement. At zero field and for $R < 3$ nm, the HFC becomes larger than twice the bulk value.[17] By considering the values of the HFC as a function of the electric field, we observe that, as the radius of the NC declines, the HFC of the ground state decreases more smoothly and becomes negligible at higher electric field values than for larger radii NCs. This trend, common to all of the NCs that we investigated, can be attributed to modification of the energy levels due to confinement.

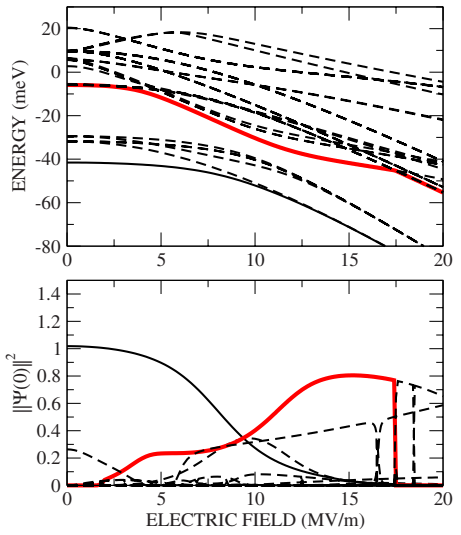

FIG. 3. (Color online) The same as Fig. 1 but for a nanocrystal with a 10 nm radius.

To introduce the notation, we briefly review the physics of bulk Si:P. Bulk silicon has six conduction-band minima ("valleys"); an electron that lies in a valley can be scattered into a different valley by the potential that is generated by the P impurity. This effect is called valley-orbit coupling.[1] If the valley-orbit coupling is neglected or if the host semiconductor has only one conduction-band minimum, the electron that is bound to an impurity shows shallow hydrogenic energy levels,[1] labeled according to conventional notation: $1s, 2s, 2p, 3s, \ldots$ For a P impurity in Si, the valley-orbit interaction couples the six $1s$ hydrogenlike states[1] (one for each the six valleys), forming the $1s$ manifold.[9] In bulk Si at zero field, the $1s$ manifold has the following energy levels in order of increasing energy (labeled according to symmetry): a singlet ($A_1 = -45.5$ meV, the ground state), a triplet ($T_2 = -33.8$ meV), and a doublet ($E = -32.6$ meV). The experimental energy levels of Si:P bulk have been reproduced by the approach that was used in the present work ($A_1 = -41.7$ meV, $T_2 = -32.3$ meV, and $E = -30.1$ meV).[10] In fact, the differences between the theoretical and experimental data for the energies of the $1s$ manifold were ~ 4 meV or less. This value also provides an estimation of the numerical accuracy of our calculation (see Ref. 17 for a discussion of the effect of confinement in NC at zero field). The degeneracy of the E states and, partially, of the T_2 states is removed by the effect of the electric field, as shown in the top panels of Figs. 1–4 in which the five distinct energy levels (one doubly degenerate) of the $1s$ manifold and their modification under the effect of the electric field are patent, at least for smaller NCs among the ones that are shown [solid and dashed black lines below the solid red (gray in black and white) thick line].

We begin by discussing the case of NC for which $R = 20$ nm. In Fig. 1, from zero to 3–4 MV/m, the energies of the $1s$ manifold as a function of the electric field are modified by merely several percentage points. At variance, the energies of the $2p$ manifold in general show a more pro-

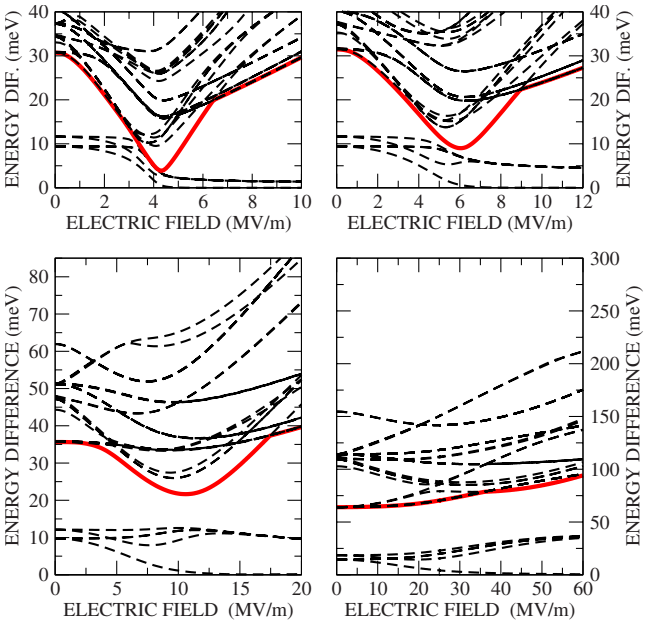

FIG. 5. (Color online) Difference between the energy of the excited states and the energy of the ground state for nanocrystals with $R=20$ nm (top-left panel), $R=15$ nm (top-right panel), $R=10$ nm (bottom-left panel), and $R=5$ nm (bottom-right panel). The zero on the vertical axis denotes the ground state, a (red) thick solid line denotes the lower energy level of the $2p$ manifold, and dashed (black) lines denote the other energy levels.

nounced dependence on the electric field. In fact, when a field of 3–4 MV/m is applied, some energy levels of the $2p$ manifold (and, in particular, the ones that originate from the $2p_0$ levels) show energies that are comparable with those of the $1s$ manifold. This phenomenon is similar to that predicted in the bulk at a considerably lower electric field, 2.5 MV/m,[10] and disappears progressively as the NC radius becomes smaller.

Because, according to Fig. 1, the primary change in the HFC as a function of the electric field appears to be related to the coupling of the $1s$ and $2p$ manifolds, we considered the difference between the energy of the excited states and the ground state. A plot of this difference as a function of electric field is shown in Fig. 5 for NCs of different sizes (the zero of the vertical axis corresponds to the ground state). The solid red line denotes the lower energy level of the $2p$ manifold.

In the top-left panel of Fig. 5 (for NCs that have 20 nm radius), we see that with electric field values between 3 and 4.5 MV/m, the anticrossing of the $1s$ and $2p$ manifolds is significant. In this range of electric fields, the energies of the higher states of the $1s$ manifold and the lower state of the $2p$ manifold (namely, the $2p_0$-like state) are close, resulting in significant anticrossing among the states of the two manifolds. This anticrossing is reduced at $R=15$ nm, and it is very small at $R=10$ nm, at which the minimum difference in energy between the two manifolds (at 10.6 MV/m) is approximately 20 meV. At variance, due to confinement, with $R=5$ nm the two manifolds are completely decoupled. At $R_{sp}\sim 7$ nm, we can fix the smaller radius for which the two manifolds show anticrossing. This radius corresponds to the NC size at which the lower energy level of the $2p$ manifold has, at zero field, an energy that is comparable with the bottom of the conduction band of Si (Ref. 17) (for an NC that has a smaller radius, the energy of the $2p$ manifold is larger).

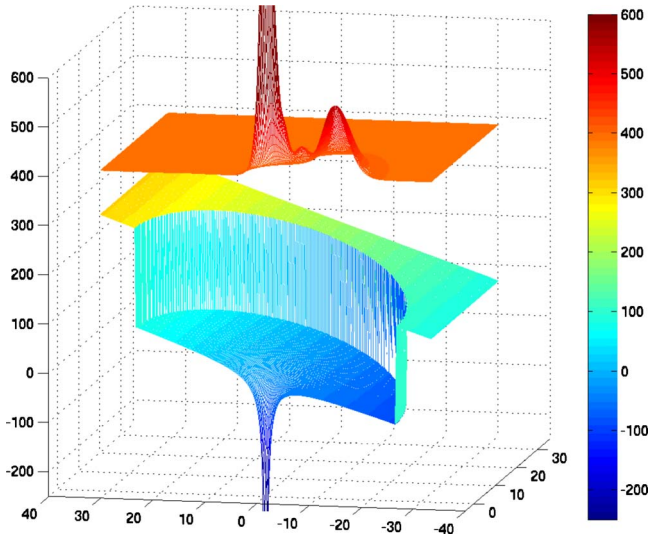

FIG. 6. (Color online) Lower surface: potential at the critical field of a P-doped Si nanocrystal with a 25 nm radius. The P atom is located at (0,0) of the horizontal plane. Upper surface: the electron density of the corresponding ground state. In the figure, the barrier height is reduced to 0.2 meV to improve readability.

The decoupling of the two manifolds can be understood easily as an effect of the confinement. If the electron is excited from the ground state into one of the $2p$-manifold states, its average distance from the P atom exceeds that of an electron in the $1s$-manifold orbits. When the NC size becomes comparable with the radius of the electronic orbital of a given state, the energy of that state is increased by the confinement.[17] Because the electronic orbitals of $2p$ states have higher energies than electronic orbitals of $1s$ states, the rise in energy due to the confinement is greater for the former and the difference in energy between the two manifolds increases as the NC radius declines. That the two manifolds are coupled for $R>R_{sp}$, at least partially, has important implications for the possibility that a hybrid state forms between the $1s$-like state and a $2p$-like state, as shown in the next section.

IV. CONFINEMENT EFFECT ON CRITICAL AND HYBRIDIZATION FIELDS

A. Definition of impurity well and surface well

If one applies an electric field of adequate magnitude within the potential barrier delimiting the NC, the sum of the impurity potential plus the electric field potential forms a double well: one well is determined primarily by the impurity potential and is centered at the P site, and the other well is determined chiefly by the electric field and the barrier at the interface between the NC and the embedding matrix. In Fig. 6 (three-dimensional plot), we sketch, as an example, the potential energy on the (100) plane that passes through the impurity, corresponding to the critical field for NCs with

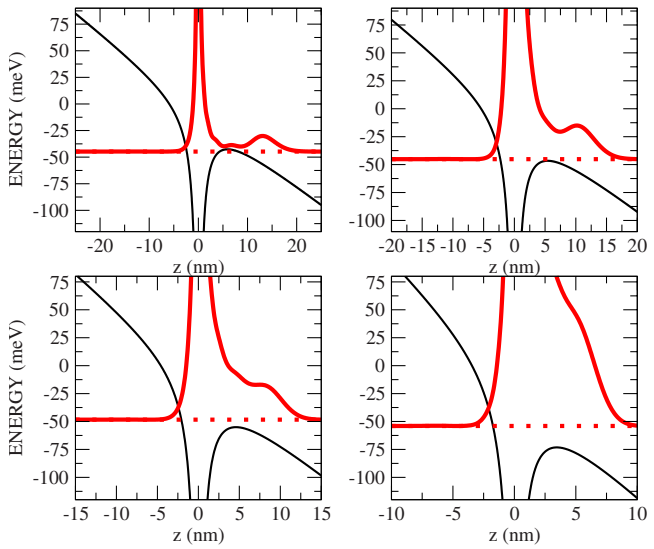

FIG. 7. (Color online) For nanocrystals of $R=25$ nm (top-left panel), $R=20$ nm (top-right panel), $R=15$ nm (bottom-left panel), and $R=10$ nm (bottom-right panel), the potential corresponding to the critical field (black line, in millielectron volt) and the envelope function of the ground state (red thick line, arbitrary units) are plotted along the direction of the electric field. The zero on the vertical scale of the envelope function corresponds to the energy of the ground state and is denoted with a dotted (red) line.

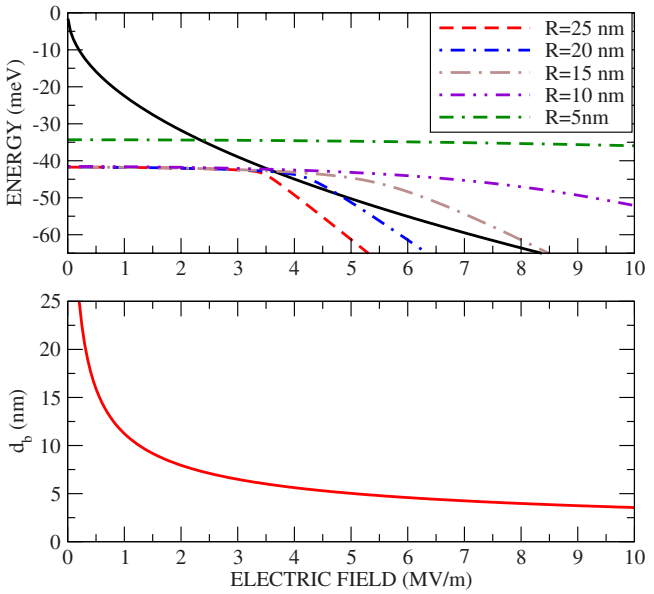

FIG. 8. (Color online) Top panel: minimum barrier height surrounding the impurity (black solid line) and ground state of P-doped NCs with different radii (dashed and dot-dashed lines) as a function of the electric field. Bottom panel: distance of the point of minimum barrier height from the impurity as a function of the electric field.

$R=25$ nm. In Fig. 7 (two-dimensional plot), we show the potential energy along the [001] direction at $\mathcal{E}_{cr}$ for NCs of different sizes. In these figures, one can distinguish the two wells that are formed by the potential within the NC radius: the "impurity well" that is centered at P and generated by V_{imp} and the electric field, and the well (with an approximately triangular section in Fig. 7) that is formed by the electric field and the potential barrier at the interface between the NC and the embedding matrix. The latter well is placed near the NC surface along the direction of the electric field, and hereafter, we refer to it as the "surface well." Between these wells there is an energy barrier with height V_b which depends on the electric field and lies at a distance d_b from the P atom along the field direction.[28]

In Fig. 8, we show the computed values of V_b and d_b as a function of the electric field (note that these values are the same as for bulk Si:P). For a given value of the electric field, if $R \leq d_b$ there is no formation of the surface well.

B. Critical and hybridization fields

In this section, we introduce the critical and hybridization fields for subsequent discussion of the physical properties of NCs. Similar to Ref. 10, we define the critical field $\mathcal{E}_{cr}$ as the electric field that corresponds to the minimum-energy difference between the lower energy level that originates from the $2p$ manifold at zero field [red (gray in black and white) solid line in the figures] and the ground state (black solid line). Similar definitions are also adopted for the case of a donor near an interface.[13] Note that, in Ref. 13 the relevant anticrossing to determine $\mathcal{E}_{cr}$ is the one that involves the lower eigenstate, while in the present work (and in Ref. 10) $\mathcal{E}_{cr}$ corresponds to the minimum difference between the lower energy level that originates from the $2p$ manifold at zero field and the ground state that originates from the $1s$ manifold at zero field.

In bulk Si:P, for fields that are lower than $\mathcal{E}_{cr}$, the ground state corresponds to the $1s$ singlet (A_1) state and the lower state of the $2p$ manifolds corresponds to the $2p_0$-like state.[10] At $\mathcal{E}_{cr}$, the two states show anticrossing and for a field that is larger than $\mathcal{E}_{cr}$, the ground state becomes $2p$ like.

The critical field $\mathcal{E}_{cr}$ is related to the difference between the energy of the ground state and V_b. To provide evidence of this assertion, in Fig. 8 we show the ground-state energy of P-doped Si-NCs with different radii. For large NCs (see the data for $R=25$ nm in the figure), the energy of the ground state, $E_g(\mathcal{E})$, is always lower than V_b and the critical field $\mathcal{E}_{cr}$ corresponds to the electric field at which the difference between V_b and the ground-state energy is at its minimum. As the radius of the NC decreases, the difference between V_b and $E_g(\mathcal{E}_{cr})$ shrinks.

We call R_t the radius of the NC at which $E_g(\mathcal{E}_{cr})=V_b$. For NCs with $R<R_t$, there is a range of the electric fields at which $E_g(\mathcal{E})>V_b$. We define the minimum and maximum hybridization fields (for reasons that will be clarified in Sec. IV E) $\mathcal{E}_{\min}$ and $\mathcal{E}_{\max}$ as the values of the electric field at which the energy of the ground state is equal to V_b. At $R=R_t$, we have $\mathcal{E}_{\min}=\mathcal{E}_{\max}=\mathcal{E}_{cr}$; in general, for $R<R_t$ we have $\mathcal{E}_{\min}<\mathcal{E}_{cr}<\mathcal{E}_{\max}$. The reader should note in Fig. 8 that for $R=5$, 10, 15, and 20 nm, there is a range of electric fields for which the energy of the ground state is higher than V_b. For $R=10$, 15, and 20 nm, $d_b(\mathcal{E}_{\min})<R$. For NCs of this size, $\mathcal{E}_{\min}$ corresponds to a transition of the ground state from a state that is bound to the impurity to a hybrid state that comprises the impurity and the surface-well state. This phenomenon holds true for NCs that have a radius that is greater

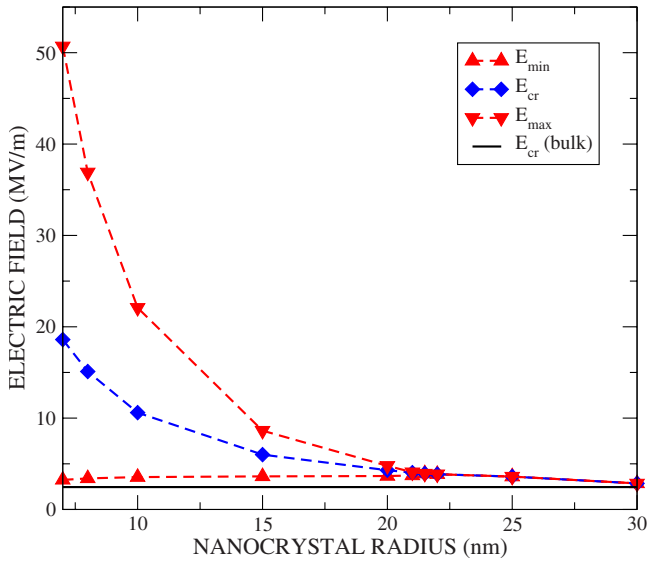

FIG. 9. (Color online) Critical field of P-doped Si nanocrystals as a function of crystal radius (diamonds). The upper ($E_{\max}$) and lower ($E_{\min}$) limits of the hybridization range are shown as downward and upward triangles, respectively. The horizontal line corresponds to the bulk value of the critical field. Dashed lines are a guide for the reader.

than $R_{dot} \equiv d_b(\mathcal{E}_{\min}) \sim 6.5$ nm. For $R < R_{dot}$, if an electric field whose magnitude is equal to $\mathcal{E}_{\min}$ is applied, there is no formation of a surface well and the ground state is confined in a one-well potential. The dependence of $\mathcal{E}_{cr}$, $\mathcal{E}_{\max}$, and $\mathcal{E}_{\min}$ as a function of NC radius is shown in Fig. 9.

C. Confined regimes

In this section we discuss how different physical regimes, due to confinement, are related to the NC radius. The effect of the anticrossing of the $1s$ and $2p$ manifolds, corresponding to $\mathcal{E}_{cr}$, has important consequences on the energy and, in particular, the wave function of the ground state. To study this aspect, we consider the envelope functions of the shallow states rather than the whole wave functions. In fact, in real space the envelope functions vary smoothly at a length scale that is comparable with the Si lattice parameter. At variance, the wave function on the same length scale shows many oscillations around the value of the envelope function. The wavelength of these oscillations is on the order of a fraction of a nanometer and it is due to the intervalley interference (this situation, for the bulk case, is well illustrated in Fig. 2 of Ref. 10 in which the envelope function and the wave function are plotted along the direction of the electric field). In the present work, we are interested in determining the probability of finding a shallow electron in different regions (surface/center) of the NC; i.e., we are interested in the change in the modulus of the wave function on the scale of the NC radius, which is on the order of nanometers. For this reason, we find it convenient to plot only the envelope function as a function of the position vector, instead of considering the whole wave function.

In Fig. 7, we show the square modulus of the ground-state envelope function (red line), computed at the critical field $\mathcal{E}_{cr}(R)$, for NCs of different sizes. In the same figure, we show the potential, which is the sum of the screened Coulomb potential and the potential that corresponds to the electric field $\mathcal{E}_{cr}$.

D. Tunneling regime

For an NC whose radius is larger than R_t (according to our results, $R_t \sim 21$ nm), we are in the tunneling regime: at the critical field, the electron in the ground state, confined around the P atom by the potential barrier that is generated by the impurity, can move via the *tunnel effect* to the surface well. In fact, as shown in the top-left panel of Fig. 7, for $R = 25$ nm, the energy of the ground state, $E_g(\mathcal{E})$, remains lower than the minimum of the energy barrier around the P atom, V_b, similar to what occurs for the P impurity in bulk Si.[10] For NCs whose size corresponds to the tunneling regime, at $\mathcal{E}_{cr}$ there are two well-resolved peaks in the envelope function. One peak is sharp and centered at the impurity site (the origin of the horizontal axis), formed primarily by $1s$ states; the other peak is smooth and centered in the well that is generated by the uniform electric field and the barrier at the interface between the NC and the embedding matrix (in the bulk case, there is no surface well but there is a free-electron region).

E. *s-p* hybridization regime

For NCs that are smaller than R_t and larger than $R_{sp} \simeq R_{dot}$, the energy of the ground state that corresponds to $\mathcal{E}_{cr}$ is higher than the energy of the impurity barrier, and the ground state forms a hybrid state between the $1s$ states that are localized around the P and the $2p$ states that are localized in the surface well. With regard to the squared modulus of the envelope function for NC with $R = 20$ nm, we observe that the peak at P and the small peak at the surface well are only partially resolved but for $R = 15$ nm, the envelope function forms an "elbow," corresponding to the surface well. At $R = 10$ nm, there is only a structure that is formed by one asymmetric peak with a "hump" on the right side due to the presence of the barrier well.

The ground state is formed by the hybridization of the $1s$ impurity states and the $2p$ surface-well states, when its energy is higher than the potential barrier, V_b, which depends on the electric field and NC radius and which separates the impurity from the surface well. Thus, $[\mathcal{E}_{\min}, \mathcal{E}_{\max}]$ defines the range in which the *s-p* hybrid states are formed. For $\mathcal{E} < \mathcal{E}_{\min}$, the energy of the ground state is lower than the potential barrier and the $1s$-like state is confined around the impurity; in contrast, for $\mathcal{E} > \mathcal{E}_{\max}$, the energy of the ground state is also lower than the potential barrier but the state is $2p$ like and confined in the surface well.

The values of $\mathcal{E}_{\min}$ and $\mathcal{E}_{\max}$, corresponding to NCs of different sizes, are shown in Fig. 9 for values of the electric field that corresponds to the *s-p* regime. We note from the figure that although $\mathcal{E}_{\min}$ is nearly constant in the range that is considered, $\mathcal{E}_{\max}$ depends strongly on the NC size and the hybridization range increases considerably as the NC radius declines. Within the *sp*-hybrid range, for fields that are lower than $\mathcal{E}_{cr}$, the wave function has predominantly an impurity

well component and for higher fields it has a surface-well component.

F. Dot regime

For NC radii that are smaller than R_{sp} the $1s$ and $2p$ manifolds are well separated in energy and there is no anticrossing. As shown in Fig. 4, for $R=5$ nm, at high electric fields (>40 MV/m) the ground state becomes nearly doubly degenerate and the remaining four states of the $1s$ manifold have similar energies (at 60 MV/m the difference in the energies of the four higher states of the $1s$ manifold is less than 2 meV). At $R=R_{ss}\sim 4$ nm, the effect of confinement also becomes significant for the excited states of the $1s$ manifold. The energy separation of the ground state (A_1) and the excited states (E,T_2) increases. At zero field, due to confinement, the excited $1s$ states have energies that are comparable with the bottom of the conduction band of Si for an NC that has a radius R_{ss} [~ 4 nm (Ref. 17)]. When $R>R_{ss}$, for low electric fields the electron in the ground state is still bound to the donor; for $R<R_{ss}$ the electron's energy is higher than the bottom of the conduction band. This situation is similar to that of an electron confined in a quantum dot. Because we expect to approach the limit of validity for the approximation that we have used in this study for $R\leq 2-3$ nm we do not discuss the latter regime further.

In summary, we can distinguish four cases according to the NC size: (I) the tunnel regime for $R>R_t\sim 21$ nm in which the ionization of the donor is made possible by a tunnel effect at a critical electric field; (II) the hybrid s-p regime for $R_{sp}<R<R_t$, where $R_{sp}\sim 7$ nm revealing a range of electric fields in which the ground state is a hybrid of $1s$ states that are localized at the impurity and $2p$ states that are localized at the NC surface well; (III) mixed $1s$-manifold states for $R_{ss}<R<R_{sp}$, with $R_{ss}\sim 4$ nm, in which the ground state is a hybrid of states of the $1s$ manifold; (IV) the "pure" dot states, for $R<R_{ss}$, the physics of which is expected to be similar to the Stark effect of an electron in a quantum dot.

V. EFFECT OF CONFINEMENT ON HYPERFINE COUPLING

Finally, we discuss the effect of confinement on HFC parameters as a function of electric field. In general (see Figs. 1–4), for a given NC radius, as the electric field increases, the HFC of the ground state decreases and the HFC of some excited state becomes significant. In particular, to set a reference, we consider the HFC that corresponds to the $2p_0$-like level (similar considerations can also be made for other excited states). For NCs that have a radius greater than R_{sp}, we find a value of the electric field $\mathcal{E}_{ex}$ at which the ground state and excited $2p_0$-like state have the same HFC value. For $R>R_t$, $\mathcal{E}_{ex}$ essentially corresponds to the critical field (it can be used as an alternative definition of $\mathcal{E}_{cr}$). For $R<R_t$, we have $\mathcal{E}_{\min}<\mathcal{E}_{ex}<\mathcal{E}_{cr}$. At $\mathcal{E}_{ex}$, the ground state and the excited states correspond to hybridization states that are formed by the impurity state and the surface-well state.

As an example, we consider an NC with $R=8$ nm. For $\mathcal{E}\sim 12.6$ MV/m, the HFC of the ground state is approximately one half of the bulk value at zero field. Notably, at this electric field value, the ground state has an HFC value that is similar to the HFC of the $2p_0$ state and to the HFC of one excited state of the $1s$ manifold—namely, one of the two levels that originated from the E states at zero field.

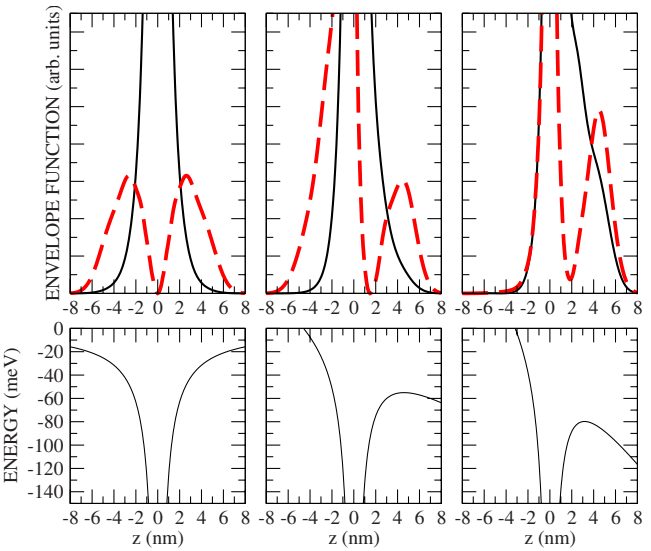

FIG. 10. (Color online) Top panels: the square modulus of the envelope function of the ground state (black line) and one of the $2p$ manifolds (red dashed line) of an Si:P nanocrystal with an 8 nm radius at three different values of electric field: zero field (left panel), 6.0 MV/m (central panel), and 12.6 MV/m (right panel). Bottom panels: for each value of the electric field the corresponding potential is plotted. The horizontal axis is directed as the electric field and zero corresponds to the P position.

The explanation of this effect is illustrated in Fig. 10, in which, for NCs with $R=8$ nm, the square modulus of the envelope function is plotted along the [001] direction for three values of the uniform electric field. In the figure, we choose the vertical scale to visualize the magnitude and symmetry with respect to the P atom of an excited state of $2p$ manifolds and the ground state ($1s$ manifold). The magnitude of the envelope function at P (not visible in the figure) is shown in the bottom panels of Fig. 11. At zero field, the envelope function of the ground state is symmetrical and peaks around the position of the P atom (corresponding to zero on the horizontal axis), and the envelope functions of a state of the $2p$ manifold vanish in correspondence to the node of the p-like wave function at the P nuclear site. Yet, due to the confinement in the NC, the electronic orbits of the $2p$ manifold are closer to the P impurities than the corresponding bulk ones. As discussed, the confinement effect is more effective for the $2p$ rather than the $1s$ manifold. As shown in Fig. 10, for $R=8$ nm, the envelope function of the state of the $2p$ manifold has a peak at zero field that is only 3–4 nm from the P atom. When a uniform electric field is applied, the envelope functions lose their symmetry around the P atom, and due to the combination of the confinement and the electric field, the peak of the $2p$—like state (at the left of the P atom in the figure) is pushed toward P while the node of the envelope (or wave) function shifts to the right by a similar amount. Consequently, by increasing the electric

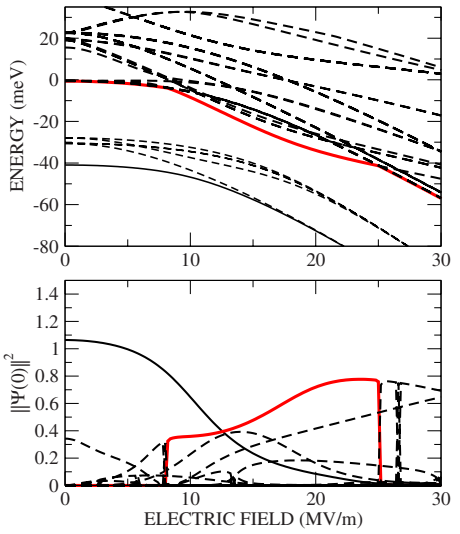

FIG. 11. (Color online) The same as Fig. 1 but for a nanocrystal with an 8 nm radius.

field, the peak of the $2p_0$—like level nears the P site and the HFC of this level increases. At approximately $\mathcal{E} \sim 12.6$ MV/m, its value is comparable with the HFC of the ground state. Because the confinement is less effective for the $1s$ manifold, the peak of the ground state is pushed away from the P site at a larger electric field. As a consequence, within the hybridization range, one can identify a value of electric field at which the ground state and one excited state have equal and non-negligible HFCs (further, for $R=8$ nm, there is an other excited state that has an HFC that is similar to that of the ground state). This effect raises the possibility of using excited states of shallow levels of P-doped Si-NCs for quantum computation, as envisaged below.

Schemes of quantum computing that involve excited states have been proposed.[29,30] Our results show that in the hybridization range, there is at least one value of the electric field at which it is possible to excite the electron from the ground state to a higher energy level, conserving the *same* HFC of the ground state. In principle, this step would allow one to transfer the quantum information to an excited state that has the same HFC of the ground state. We consider the $2p_0$ state (but one of the excited states of the $1s$ manifold also shows a similar effect) for possible application in a novel scheme of quantum computing because the $2p_0$ excited state is long lived,[2] compared with other excited electron levels of the P impurity in bulk Si (in the following discussion, we implicitly assume that the lifetime of the $2p_0$ is not drastically reduced by confinement or by electric fields of magnitude $\mathcal{E}_{ex}$).

We briefly outline a possible scheme for a transfer qubit. We consider two Si-NCs that have an equal radius, the first is doped with a P atom at the center, and the second can contain a P atom or not (the following qualitative discussion is not significantly affected by the presence of a P atom in the second dot). In the first NC, the qubit is encoded in the P nuclear spin, which is coupled to the spin of the shallow electron through the HFC.

First, the electric field is adiabatically switched on in the direction that is perpendicular to the line that passes through the centers of the two NCs. When the value of $\mathcal{E}_{ex}$ is reached, the electron is excited (photoexcited, for example) from the $1s$ ground state to the $2p_0$ state, conserving the same coupling with the nuclear spin, because, at $\mathcal{E}_{ex}$, the HFC of the ground and $2p_0$ states are the same. Second, if the electric field is adiabatically switched off in a time that is shorter than the lifetime of the $2p_0$ state, the electron will remain in the excited state, conserving the spin orientation. In this way, at zero field the electron (with the original spin orientation) is in the $2p_0$ exited state, which, for this NC size, has an energy that is equal to (or larger than) the bottom of the conduction band. As a result, at zero field the electron spin, in the $2p_0$ excited state, is decoupled from the nuclear spin (conserving the same spin orientation). Third, because an electron in an NC can be transferred to the adjacent NC by tunneling through the oxide when the NC distance is less than 2 nm,[24] the qubit that is stored to the electron spin can be transferred to the second NC.

We expect that excited states (and, in particular, the ones whose energies are higher than the bottom of the conduction band of Si-NC) have higher probabilities of tunneling into the second NC than the ground state (bound to the impurity). Therefore, we can reasonably assume that for an appropriate choice of distance between two NCs, only the electron in the excited state has a significant probability of tunneling through the oxide. This scheme can be used to adiabatically decouple nuclear and electron spin and transfer the qubit that is stored in the electron spin from one NC to the adjacent one. Our proposal constitutes an alternative to the use of the oxide barrier film, which is typically assumed[3,19] in the implementation of Kane-type schemes for quantum computing.

VI. SUMMARY

In summary, we have computed the effect of confinement in P-doped Si-NCs in the presence of a uniform electric field. We can distinguish four cases according to NC size: (I) tunnel regime, for $R > R_t \sim 21$ nm, in which the ionization of the donor is made possible by tunnel effect at a critical electric field; (II) hybrid s-p regime for $R_{sp} < R < R_t$, with $R_{sp} \sim 7$ nm—in this regime, there is a range of electric fields in which the ground state is a hybrid of $1s$ states that are localized at the impurity and a $2p$ state that is localized at the surface well at the interface; (III) mixed $1s$-manifold states for $R_{ss} < R < R_{sp}$, with $R_{ss} \sim 4$ nm, at which the ground state is a hybrid of states of the $1s$ manifold; and (IV) pure dot states, for $R < R_{ss}$, the physics of which is expected to be similar to the Stark effect of electrons in a quantum dot. A scheme for transferring qubits from one NC to an adjacent one using excited states has been proposed and discussed.

[1] See, e.g., P. Y. Yu and M. Cardona, *Fundamentals of Semiconductors* (Springer, Berlin, 1996) (and references therein).
[2] H.-W. Hübers, S. G. Pavlov, and V. N. Shastin, Semicond. Sci. Technol. **20**, S211 (2005).
[3] B. E. Kane, Nature (London) **393**, 133 (1998).
[4] D. Loss and D. P. DiVincenzo, Phys. Rev. A **57**, 120 (1998).
[5] C. I. Pakes, C. J. Wellard, D. N. Jamieson, L. C. L. Hollenberg, S. Prawer, A. S. Dzurak, A. R. Hamilton, and R. G. Clark, Microelectron. J. **33**, 1053 (2002).
[6] G. D. J. Smit, S. Rogge, J. Caro, and T. M. Klapwijk, Phys. Rev. B **68**, 193302 (2003).
[7] H. Overhof and U. Gerstmann, Phys. Rev. Lett. **92**, 087602 (2004).
[8] G. D. J. Smit, S. Rogge, J. Caro, and T. M. Klapwijk, Phys. Rev. B **70**, 035206 (2004).
[9] M. Friesen, Phys. Rev. Lett. **94**, 186403 (2005).
[10] A. Debernardi, A. Baldereschi, and M. Fanciulli, Phys. Rev. B **74**, 035202 (2006).
[11] L. M. Kettle, H.-S. Goan, S. C. Smith, C. J. Wellard, L. C. L. Hollenberg, and C. I. Pakes, Phys. Rev. B **68**, 075317 (2003).
[12] A. S. Martins, R. B. Capaz, and B. Koiller, Phys. Rev. B **69**, 085320 (2004).
[13] M. J. Calderón, B. Koiller, and S. Das Sarma, Phys. Rev. B **77**, 155302 (2008).
[14] M. J. Calderón, A. Saraiva, B. Koiller, and S. Das Sarma, J. Appl. Phys. **105**, 122410 (2009).
[15] A. L. Saraiva, M. J. Calderón, X. Hu, S. Das Sarma, and B. Koiller, Phys. Rev. B **80**, 081305(R) (2009).
[16] T.-L. Chan, M. L. Tiago, E. Kaxiras, and J. R. Chelikowsky, Nano Lett. **8**, 596 (2008).
[17] A. Debernardi and M. Fanciulli, Solid State Sci. **11**, 961 (2009).
[18] See also A. Debernardi and M. Fanciulli, in *Electron Spin Resonance and Related Phenomena in Low Dimensional Structures*, Topics in applied Physics Vol. 115, edited by M. Fanciulli (Springer-Verlag, Berlin, 2009), pp. 221–239.
[19] B. Koiller, Nat. Phys. **4**, 590 (2008).
[20] G. P. Lansbergen, R. Rahman, C. J. Wellard, I. Woo, J. Caro, N. Collaert, S. Biesemans, G. Klimeck, L. C. L. Hollenber and S. Rogge, Nat. Phys. **4**, 656 (2008).
[21] M. Fujii, A. Mimura, S. Hayashi, Y. Yamamoto, and K. Murakami, Phys. Rev. Lett. **89**, 206805 (2002).
[22] M. Perego, M. Fanciulli, and C. Bonafos, Nanotechnology **21**, 025602 (2010).
[23] Theoretical calculation considering NC with cubic shape can also be found in literature, see, e.g., D. Ahn, J. Appl. Phys. **98**, 033709 (2005); P. Harrison, *Quantum Wells, Wires and Dots: Theoretical and Computational Physics of Semiconductor Nanostructures*, (Wiley, New York, 2005), and references therein.
[24] E.-C. Cho, S. Park, X. Hao, D. Song, G. Conibeer, S.-C. Park, and M. A. Green, Nanotechnology **19**, 245201 (2008).
[25] R. J. Powell, J. Appl. Phys. **41**, 2424 (1970).
[26] Strictly speaking this is proved to be valid for NC with radii up to 3 nm, that is, the larger size considered in Ref. 16. However, we can reasonably assume also for NCs of larger size that the configuration with P located in the central region of the NC is energetically favored with respect to the one with P close to the NC surface.
[27] An excellent introduction to envelope-function techniques can be found, e.g., A. M. Stoneham, *Theory of Defects in Solids* (Oxford University Press, Oxford, 2001).
[28] Actually, V_b corresponds to a saddle point of the potential energy: it is the maximum of the potential from P to the surface well along the field direction (see Fig. 7) and it is the lower value of the energy of the barrier delimiting the impurity well.
[29] A. M. Stoneham, A. J. Fisher, and P. T. Greenland, J. Phys.: Condens. Matter **15**, L447 (2003).
[30] A. Kerridge, A. H. Harker, and A. M. Stoneham, J. Phys.: Condens. Matter **19**, 282201 (2007).